Mosaic-like Monolayer of Graphene Oxide Sheets Decorated with Tetrabutylammonium Ions

Jung Woo Kim,[†] Dongwoo Kang,[†] Tae Hyeong Kim,[‡] Sung Guk Lee,[‡] Nami Byun,[‡] Dong Wook Lee,[‡] Byung Hwa Seo,[‡,⊥,*] Rodney S. Ruoff,[§] and Hyeon Suk Shin[†,*]

[†]Interdisciplinary School of Green Energy and Low Dimensional Carbon Materials Center, Ulsan National Institute of Science & Technology (UNIST), UNIST-gil 50, Ulsan 689-805, Korea, [‡]LG Electronics Advanced Research Institute, Materials and Components Laboratory, Baumoe-ro 38, Seocho-gu, Seoul 137-724, Korea, and [§]Department of Mechanical Engineering and the Materials Science and Engineering Program, The University of Texas, Austin, Texas 78712, United States. [⊥]Present address: Department of Materials Science and Engineering, University of Illinois, Urbana, Illinois 61801, United States.

ABSTRACT We report the fabrication of mosaic-like monolayers of graphene oxide (G-O) coated with tetrabutylammonium ions (TBA) using a simple spin-coating method. The TBA-coated G-O (TG-O) sheets were prepared by "spontaneous exfoliation" of graphite oxide intercalated with tetrabutylammonium hydroxide (TBAOH) in the wet state, without the need for sonication. Mosaic-like monolayers could be formed on a variety of substrates such as Si wafer (coated with the thin native oxide), SiO_2/Si wafer, graphene grown by chemical vapor deposition and then transferred on SiO_2/Si wafer, Au film on Si wafer, and Cu foil. The mosaic-like monolayer of TG-O was compared with monolayers of G-O and TG-O prepared using a Langmuir–Blodgett (LB) trough. The formation of the mosaic-like TG-O monolayer films was attributed to (1) weakening of the electrostatic repulsion between G-O sheets by TBA, and (2) prevention of the overlap and stacking of TG-O sheets by disruption of the hydrogen bonding between the basal plane of one sheet and the basal plane or edge of another, by adsorbed TBA. External reflection FTIR spectroscopy showed that spectral features of the mosaic-like monolayer of TG-O made by simple spin-coating were the same as those for the monolayer fabricated using the LB assembly, indicating the same spatial orientations of functional groups. This study provides a very simple route to a complete monolayer of G-O without the need for an LB trough.

KEYWORDS: graphene oxide · graphite oxide · monolayer · mosaic-like film · tetrabutylammonium hydroxide · Langmuir–Blodgett (LB) film

Graphene is considered to be a promising material for a variety of applications owing to its outstanding electrical, chemical, optical, and mechanical properties.[1−5] There are many methods that can be used to synthesize graphene, including mechanical exfoliation,[1] chemical conversion,[6,7] epitaxial growth,[8,9] and chemical vapor deposition (CVD).[10] One chemical conversion approach gives graphene oxide (G-O) and reduced graphene oxide (rG-O), *via* the initial preparation of graphite oxide from graphite, and is perceived to be a cost-efficient and scalable method. Graphite oxide can be easily dispersed in H_2O due to its many oxygen-containing functional groups to yield individual G-O sheets. However, the exfoliation to single layer sheets (here referred to as G-O and rG-O) on a large scale is an ongoing challenge.[11,12] Intercalation of large molecules into graphite oxide has been used to increase the interlayer spacing between sheets to allow more complete exfoliation by weakening the (primarily H-bonding) interactions between the layers.[13−15] Surfactant molecules such as alkylamine have been used as intercalants.[13,16,17]

The pursuit of large-scale G-O or rG-O films has included methods such as vacuum filtration,[7,17−19] dip coating,[20,21] spin-coating,[22−25] layer-by-layer (LbL) deposition,[26,27] and Langmuir–Blodgett (LB) assembly.[27,28] The LB assembly approach has been shown to be suitable for forming a monolayer of G-O. G-O sheets float on the surface of water and form a monolayer without the need for stabilizing agents such as surfactants. This has been rationalized in terms of the G-O sheets

* Address correspondence to shin@unist.ac.kr, bhseo@illinois.edu.

Received for review July 2, 2013 and accepted August 21, 2013.

Published online August 21, 2013
10.1021/nn403363s

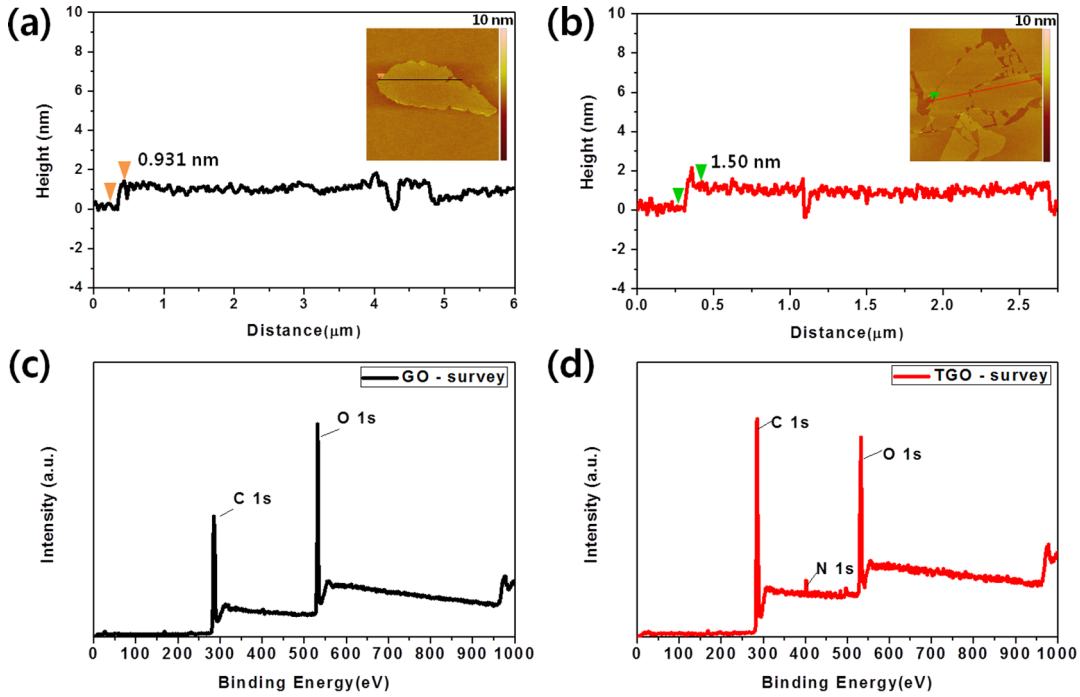

Figure 1. Height profiles of G-O (a) and TG-O (b) from AFM images in the insets. XPS survey spectra of G-O film (c) and TG-O film (d).

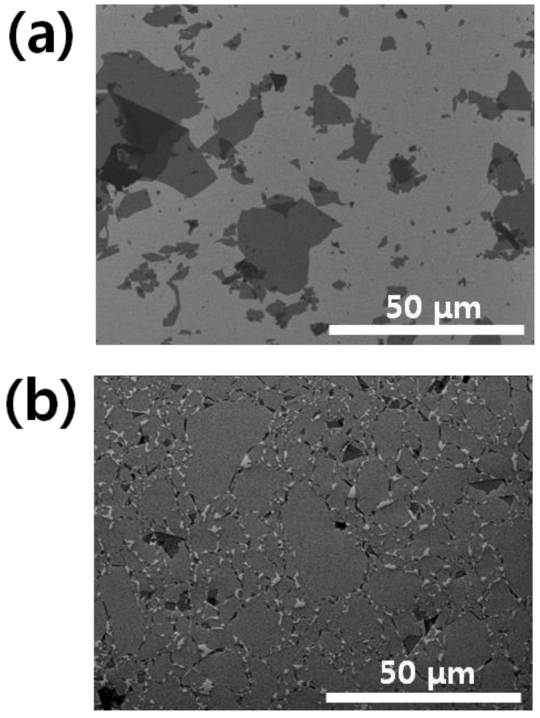

Figure 2. SEM images of (a) spin-coated G-O film and (b) TG-O film, each on SiO_2 (300 nm)/Si wafer.

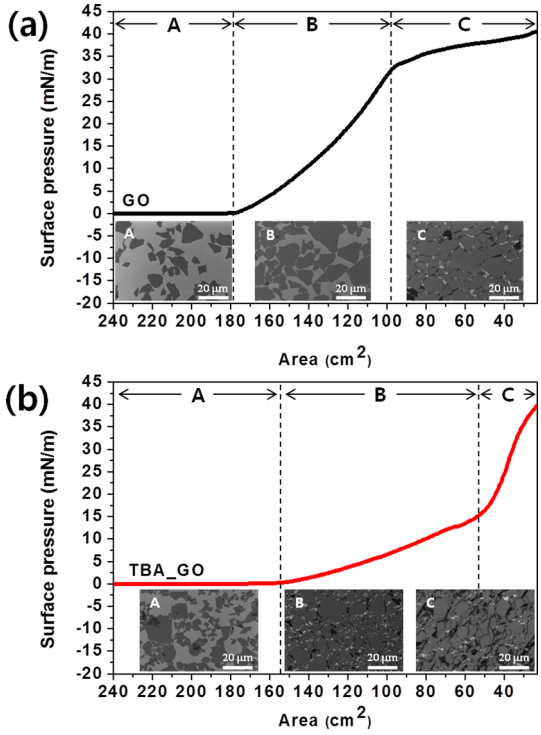

Figure 3. Surface pressure–area isotherms of (a) G-O and (b) TG-O. Insets are SEM images of G-O and TG-O layers transferred onto SiO_2 (300 nm)/Si substrates at different stages of isothermal compression.

having a mixture of hydrophobic and hydrophilic regions in the basal plane, and hydrophilic edges.[28] At the air–water interface, negatively charged G-O sheets pack under the applied LB pressure due in part to intersheets repulsion; such repulsion prevents the sheets from forming overlapping layers during compression in the LB trough, and the resulting G-O monolayer can then be transferred to a solid substrate.[27] One disadvantage of the LB assembly is that the 'Langmuir film' on water is sensitive to external

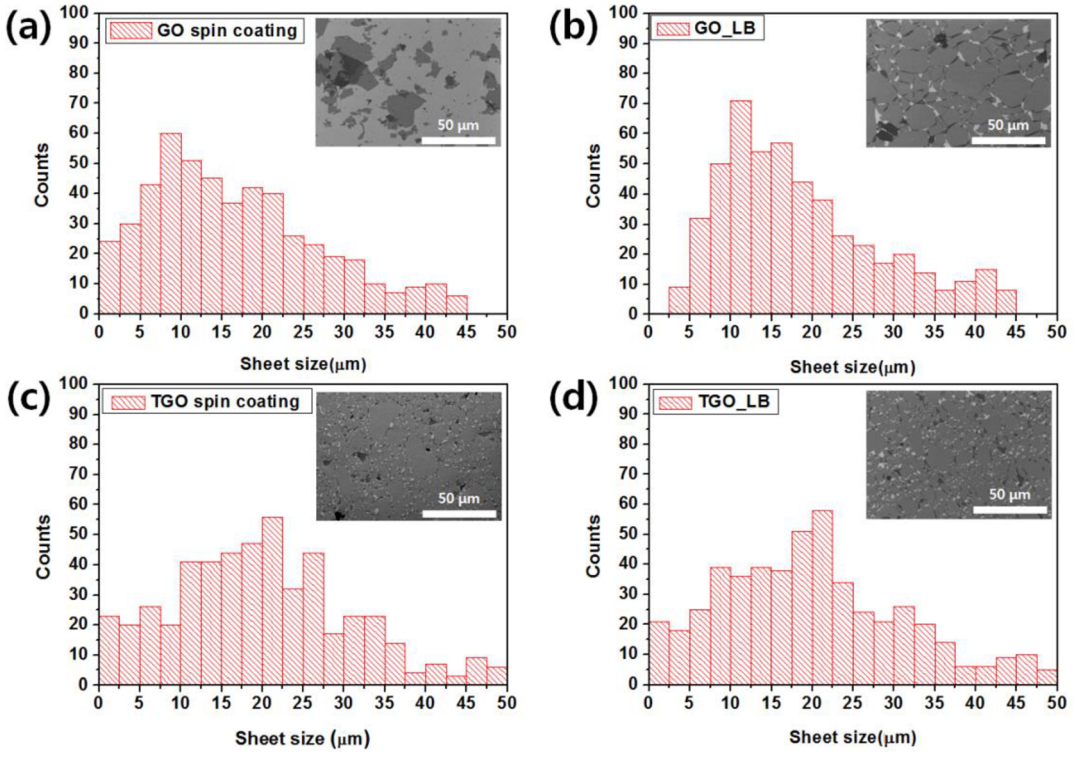

Figure 4. Histograms of sheet size distributions of GO films fabricated by (a) spin coating and (b) LB trough and TGO films fabricated by (c) spin-coating and (d) using an LB trough.

influences such as temperature, aging, and pressure. The LB assembly also requires expensive equipment and is extremely slow.

By simply spin-coating a tetrabutylammonium (TBA)-treated G-O solution ('TG-O' solution), in this study, mosaic-like monolayers of G-O on a variety of substrates were prepared and compared with TG-O films formed using LB assembly and with those consisting of only G-O sheets made by each method.

RESULTS AND DISCUSSION

Intercalation of large molecules into graphite oxide has been used to obtain intercalated graphite oxide with large interlayer spacing, in high yield.[29] Tetrabutylammonium hydroxide (TBAOH) has often been used as an intercalant to increase the interlayer spacing of layered materials.[13,14,28−31] In this study, single layers of graphite oxide, referred to here as G-O sheets, coated with TBA, were prepared by soaking graphite oxide in an aqueous solution of TBAOH. No special exfoliation step (such as sonication) was required to obtain these G-O sheets. In general, sonication causes the G-O sheets to break down into small pieces.[32] Thus, this study did not employ any exfoliation step like sonication, even though the yield of obtaining single layer sheets is low without an exfoliation step. The coating of G-O with TBA was evaluated by monitoring the change in thickness using atomic force microscopy (AFM) and assessing the nitrogen signal in the X-ray photoelectron spectroscopy (XPS) spectrum (Figure 1). The thickness of the G-O layers was measured to be about 0.93 nm, consistent with the thickness values reported in the literature.[33−35] The thickness of TG-O sheets was found to be about 1.50 nm. This difference in thickness is similar to the 0.47 nm thickness of TBA when in the flattened conformation.[36] In addition, in contrast to the XPS spectrum of GO in Figure 1c, that of the TG-O film, Figure 1d, shows an N 1s peak of considerable intensity. The yield of single-layer, *i.e.*, G-O sheets obtained from the graphite oxide gel, was found to be 46% when TBA was used as an intercalant, but only 18% in the absence of an intercalant (Table S1). It should also be noted that the yield of single-layer, *i.e.*, G-O sheets obtained from graphite oxide in a gel state, was 8% higher than that obtained from the materials in the dry state (Table S1). This indicates that graphite oxide in the gel state (instead of drying the graphite oxide solution) should be used to increase the yield of single layers. The X-ray diffraction (XRD) spectrum of graphite oxide in the gel state did not show the (002) peak that would be caused by stacking of G-O layers (Figure S1). Therefore, graphite oxide in the gel state was used in this study.

We found that the TG-O forms a well-packed, 'mosaic-like' monolayer on a variety of substrates, including Si wafer, CVD-grown graphene, Cu foil, and Au/Si surfaces, as shown in Figure S2. Figure 2 shows scanning electron microscopy (SEM) images of G-O and TG-O films that were prepared by spin-coating. The G-O sheets in Figure 2a can be seen to be randomly

distributed; whereas, the TG-O sheets formed a densely packed monolayer where 'puzzle pieces' closely fit together with only small gaps in the film. The TG-O film appears very similar to reported LB monolayers of G-O.[27,28] The well-packed monolayer of TG-O sheets was also confirmed by measuring the sheet resistance. The resistance of a TG-O film formed by carrying out the spin-coating process twice and annealing at 900 °C was found to be 32.2 kΩ/□ at 96% transmittance. The measured sheet resistance is lower than that of recent studies, the values of which were in the range of 74−260 kΩ/□ and which were also evidently for thicker films (around 93% transmittance),[20,24,26,28,37] indicating that TG-O forms particularly well-packed, thin layers. While not suitable for transparent conducting electrodes, the TG-O film may benefit applications requiring very thin and uniform films.

Since the TGO sheets formed a mosaic-like monolayer, it was relevant to compare them with monolayer films produced using LB trough methods. Surface pressure−area isotherms were measured to investigate the interactions between the G-O or TG-O sheets (Figure 3). The G-O and TG-O monolayers were transferred to substrates at various points during compression, and their SEM images are shown in the insets of Figure 3. As the area was decreased by the compression, the separation between sheets decreased, and the surface pressure increased. This increase has been attributed to the strong edge-to-edge electrostatic repulsion between carboxylate anions on the edges of neighboring sheets.[38]

The isotherm of G-O has three regions (Figure 3a). In the region of 240−180 cm^2, the surface pressure is 0 mN/m, indicating that neighboring G-O sheets were not yet interacting. The surface pressure increased steadily for 180−97 cm^2. Below 97 cm^2, the G-O sheets have formed a monolayer. This G-O isotherm pattern is consistent with other studies.[27,28,38] The isotherm of TG-O also consists of three regions. Up to 156 cm^2, the surface pressure is 0 mN/m. Between 156 and 53 cm^2, the TG-O sheets formed a monolayer, and then below 52.98 cm^2, overlapping occurred. The surface pressure to form monolayers of G-O and TG-O was found to be over 33.4, and between 0.1 and 15.7 mN/m, with areas of less than 97 cm^2, and between 53 and 156 cm^2, respectively. Although the same volumes and concentrations of G-O and TG-O solutions were used, the TG-O monolayer occurred at much lower surface pressure than the G-O monolayer. This suggests that electrostatic repulsion between neighboring TG-O sheets is weaker than that between neighboring G-O sheets, which is possibly due to charge compensation of G-O by TBA molecules. The ζ-potentials of aqueous dispersions of G-O and TG-O gave values of −66.28 mV at pH 3.4 (G-O) and −49.85 mV (TG-O) at pH 6.4(Figure S3). The ζ-potential of the TG-O sheet solution was slightly greater than that of the G-O sheets, which was

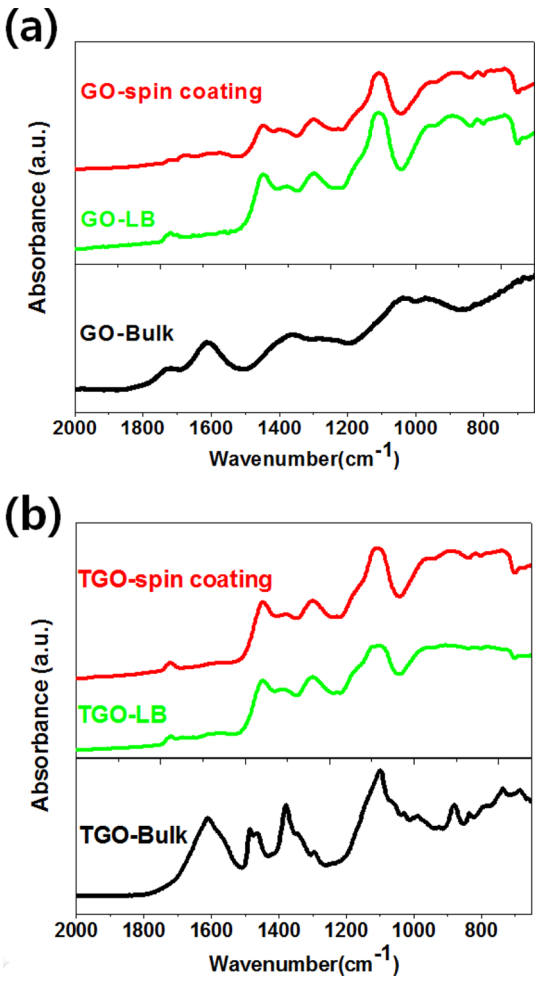

Figure 5. FTIR reflection−absorption spectra of (a) G-O and (b) TG-O films on Au substrates.

attributed to adsorption of cationic TBA molecules, which have hydrophobic alkyl groups. Furthermore, contact angle measurements of G-O and TG-O films showed TG-O was more hydrophobic than G-O, with angles of 39° and 45.5° found for thick G-O and TG-O films, respectively (Figure S4). The ζ-potential and contact angle measurements along with the aforementioned AFM and XPS results indicate that TBA molecules adhere to the G-O sheets and thus weaken the electrostatic repulsion between them. In addition, the adsorption of TBA onto G-O sheets made the TG-O sheets slightly hydrophobic, possibly due to the short alkyl chains.

The SEM images of TG-O and G-O films in the insets of Figure 3 demonstrate noticeable morphological differences between the two materials. The LB film of TG-O is composed of a combination of large and small sheets, whereas that of G-O contained only large sheets. The difference in the size distribution of G-O and TG-O films prepared by spin-coating and LB is shown in Figure 4. It can be seen that no sheets below 2.5 μm were observed for the LB film of G-O. It has been reported that the smaller G-O sheets are too

hydrophilic to float at the air–water interface, and instead dissolve and sink into water.[38] In contrast, the LB film of TG-O includes small sheets as their increased hydrophobicity due to the alkyl chains of the TBA evidently allows them to float at the air–water interface.

What drives the tiling by large and small TG-O sheets in the spun-coat and LB assembled monolayer films? As mentioned above, Figure 3b, the LB isotherm suggests edge-to-edge repulsion between sheets is weakened by the adsorption of TBA. The disruption of hydrogen bonding between the basal plane of one sheet and the basal plane or edge of another sheet by the TBA coating favors monolayer *vs* multilayer films. On the other hand, spun-coated G-O films had a greater fraction of overlapping G-O sheets (Figure S5).

FTIR reflection–absorption spectra were measured to try to learn about the orientations of functional groups in the TG-O and G-O films formed by spin-coating and LB assembly (Figure 5). The FTIR reflection–absorption spectroscopy technique is known to be very useful to estimate orientations of functional groups in thin films like a LB monolayer on metal substrates.[39,40] In the FTIR reflection–absorption spectra, bands with vibrations of dipole moments perpendicular to the metal substrate are observed, whereas those parallel to the metal surface are not observed. For the G-O film prepared by drop-casting (bulk G-O), there is a strong band at 1620 cm^{-1} due to the C=C stretching vibration; however, this almost disappears in the spectrum of the G-O LB film, indicating that the basal plane was parallel to the substrate in the LB film. The C=O stretching mode at 1722 cm^{-1} is observed for the LB film, although with a significant decrease in intensity compared to the bulk GO. This indicates that the C=O bond was not perfectly parallel to the substrate. The C=C and C=O stretching bands in the spectrum of the spin-coated G-O film slightly differs from that of the LB film, possibly because it did not form a well-packed monolayer, but rather contained some areas of overlap or aggregation. In the case of the TG-O films, the spectral features of spin-coated and LB films are the same. This indicates that the simple spin-coating of the TG-O solution afforded a well-packed, mosaic-like monolayer, which was essentially the same as that formed using the LB method. It is therefore easy to produce such monolayers without the requirement for complicated equipment such as an LB trough.

CONCLUSION

Coating G-O sheets with TBA allows simple spin-coating of extremely well tiled "mosaic-like" films on various substrates. It is suggested that the TBA coating layer strongly reduces the electrostatic repulsion between the G-O sheets and inhibits H-bonding between them. This method affords large area films of well-tiled monolayers by the simple and fast solution process using spin coating without any complicated and time-consuming process like the LB assembly.

EXPERIMENTAL METHODS

Materials. Natural graphite with an average particle size of 74 μm was purchased from Bay Carbon (Bay City, MI). Chemical reagents used for the synthesis of graphite oxide, including P_2O_5 and $KMnO_4$, were purchased from Sigma-Aldrich. H_2SO_4 was obtained from Merck Chemicals (Darmstadt, Germany). TBAOH was purchased from Sigma-Aldrich. The molecular weight cutoff (MWCO) of the dialysis tubing (Spectra/Por dialysis membrane) was 12–14 kDa.

Preparation of Graphite Oxide. Graphite oxide was prepared from purified natural graphite (SP-1, Bay Carbon) by the modified Hummers' method.[6] The graphite powder (20 g) was added to a solution of concentrated H_2SO_4 (30 mL), $K_2S_2O_8$ (10 g), and P_2O_5 (10 g) at 80 °C. The resultant dark blue mixture was thermally isolated and allowed to cool to room temperature over a period of 6 h. The mixture was then carefully diluted with distilled H_2O, filtered, and washed on the filter until the pH of the H_2O washings became neutral. The product was air-dried at ambient temperature overnight. This preoxidized graphite was then subjected to oxidation by the Hummers' method. The preoxidized graphite powder (20 g) was added to cold concentrated H_2SO_4 (460 mL). $KMnO_4$ (60 g) was then added gradually under stirring, with the temperature maintained below 20 °C throughout. The mixture was stirred at 35 °C for 2 h, and distilled H_2O (920 mL) was then added. After 15 min, the reaction was terminated by the addition of a large volume of distilled H_2O (2.8 L) and a 30% H_2O_2 solution (50 mL), resulting in a color change to bright yellow. The mixture was filtered and then washed with a HCl/H_2O solution (5 L, 1:10 v/v) in order to remove metal ions. The graphite oxide product was suspended in distilled H_2O to give a viscous, brown dispersion, which was subjected to dialysis to completely remove metal ions and acid. The mixture was subsequently centrifuged to produce the graphite oxide in the form of a gel. The final product was kept in the dark until further use.

Intercalation Reaction and Exfoliation. The graphite oxide gel (20 mg) was soaked in TBAOH/H_2O (20 mL, 1:3 v/v) for 3 days. It was then dialyzed for 2 days, and separated by centrifugation. The supernatant consisted of the TGO of single layer, which was exfoliated from TBA-intercalated graphite oxide

Spin Coating. The SiO_2 substrate (1 × 1 cm^2) was cleaned using piranha solution in order to remove any organic contamination, and then treated with O_2 plasma to produce a hydrophilic surface. A solution of TGO or GO (0.85 mg/mL) was dropped onto the substrate, which was loaded onto the stage of a spin coater (ACE-200, Dong Ah Tech), maintained for 2 min as a waiting period, and then spun at 3000 rpm for 30 s. Note that TG-O monolayers could be also formed in the concentration range of TG-O solution from 0.78 to 0.95 mg/mL and in the spin speed range from 1000 to 4000 rpm.

LB Films. Deionized water was used as the supporting subphase. When solutions of either G-O or TG-O were directly applied to the water surface, most of the sheets sank owing to the high dispersibility of the materials in aqueous solution. Commonly used hydrophobic spreading solvents, such as chloroform or toluene, were not suitable as they are not able to sufficiently disperse G-O. Methanol, however, is able to yield a stable solution,[38] and enables good dispersion and rapid spreading on the surface of water. Methanol was added to each solution to a final ratio of 1:5. The mixture was subsequently centrifuged at 3500 rpm for 10 min to remove aggregates. The LB trough (KN 2002, Nima Tech) was carefully cleaned and then filled with deionized water. The mixture (1.5 mL) was slowly dropped onto the surface of water at a rate of 100 μL/min.

Surface pressure was monitored using a tensiometer attached to a Wilhelmy plate. The film was compressed by barriers at a speed of 20 cm^2/min. Initial isotherms were taken after the film was allowed to equilibrate for at least 20 min after spreading. Isotherms in the figure have a zeroed baseline. The film was transferred to substrates at various points during the compression by vertically dipping the O_2 plasma treated SiO_2 substrate into the trough and slowly pulling it upward out of the solution (2 mm/min).

Measurements and Characterization. The interlayer spacing of the graphite oxide and TBA-intercalated graphite oxide was measured using XRD (Bruker). The morphology and sheet size of the G-O and TG-O were measured using scanning electron microscopy (SEM; FEI). The thicknesses of the monolayers of G-O and TG-O on the SiO_2 substrate were measured using AFM (Veeco) in tapping mode. The functional groups on the G-O and TG-O films were characterized using XPS (Thermo Fisher, K-alpha). Transmittance of the TG-O film on a quartz substrate was measured using UV−vis-NIR on a Cary 5000 (Varian). The resistance of the TG-O film consisting of different numbers of coatings on quartz was measured using the four-point probe method (AIT, CMT-SR 1000N). Surface pressure−area isotherms of G-O and TG-O were measured using KSV-NIMA Langmuir and LB troughs. The films were formed by the addition of 0.4 mg/mL solutions of G-O or TG-O (1.5 mL) to the air−water interface. The ζ-potentials of solutions of G-O and TG-O solution were measured using a Nano ZS (Malvern, U.K.). The molecular orientations of functional groups on the materials were measured using FTIR (Agilent) with a variable-angle reflectance accessory (Seagull), and p-polarized light at an angle of incidence of 82°. Films were prepared on Au substrates for measurement of FTIR reflection spectra, and as a reference, bulk samples were prepared on Au/Si substrates by drop-casting of TG-O and G-O solutions.

Conflict of Interest: The authors declare no competing financial interest.

Supporting Information Available: Yield of single-layer from graphite oxide, XRD spectra of graphite oxide in dry and gel states, SEM images of TG-O films on various substrates, ζ-potential of G-O and TG-O solutions, contact angle measurements of G-O and TG-O, and SEM images of G-O sheets by spin-coating. This material is available free of charge *via* the Internet at http://pubs.acs.org.

Acknowledgment. This work was supported by the Basic Science Research Program (2011-0013601) and a grant (Code No. 2011-0031630) from the Center for Advanced Soft Electronics under the Global Frontier Research Program through the National Research Foundation funded by the Ministry of Science, ICT and Future Planning, Korea and by a grant from the Fundamental R&D program for Core Technology of Industry (10038631) funded by the Ministry of Trade, Industry, and Energy, Korea.

REFERENCES AND NOTES

1. Novoselov, K.; Geim, A.; Morozov, S.; Jiang, D.; Zhang, Y.; Dubonos, S.; Grigorieva, I.; Firsov, A. Electric Field Effect in Atomically Thin Carbon Films. *Science* **2004**, *306*, 666–669.
2. Geim, A. K.; Novoselov, K. S. The Rise of Graphene. *Nat. Mater.* **2007**, *6*, 183–191.
3. Lee, C.; Wei, X.; Kysar, J. W.; Hone, J. Measurement of the Elastic Properties and Intrinsic Strength of Monolayer Graphene. *Science* **2008**, *321*, 385–388.
4. Balandin, A. A.; Ghosh, S.; Bao, W.; Calizo, I.; Teweldebrhan, D.; Miao, F.; Lau, C. N. Superior Thermal Conductivity of Single-Layer Graphene. *Nano Lett.* **2008**, *8*, 902–907.
5. Stankovich, S.; Dikin, D. A.; Dommett, G. H. B.; Kohlhaas, K. M.; Zimney, E. J.; Stach, E. A.; Piner, R. D.; Nguyen, S. T.; Ruoff, R. S. Graphene-Based Composite Materials. *Nature* **2006**, *442*, 282–286.
6. Hummers, W. S.; Offeman, R. E. Preparation of Graphitic Oxide. *J. Am. Chem. Soc.* **1958**, *80*, 1339–1339.
7. Li, D.; Muller, M. B.; Gilje, S.; Kaner, R. B.; Wallace, G. G. Processable Aqueous Dispersions of Graphene Nanosheets. *Nat. Nanotechnol.* **2008**, *3*, 101–105.
8. Berger, C.; Song, Z.; Li, T.; Li, X.; Ogbazghi, A. Y.; Feng, R.; Dai, Z.; Marchenkov, A. N.; Conrad, E. H.; First, P. N.; *et al.* Ultrathin Epitaxial Graphite: 2D Electron Gas Properties and a Route toward Graphene-Based Nanoelectronics. *J. Phys. Chem. B* **2004**, *108*, 19912–19916.
9. Rollings, E.; Gweon, G.-H.; Zhou, S.; Mun, B.; McChesney, J.; Hussain, B.; Fedorov, A.; First, P.; De Heer, W.; Lanzara, A. Synthesis and Characterization of Atomically Thin Graphite Films on a Silicon Carbide Substrate. *J. Phy. Chem. Solids* **2006**, *67*, 2172–2177.
10. Li, X.; Cai, W.; An, J.; Kim, S.; Nah, J.; Yang, D.; Piner, R.; Velamakanni, A.; Jung, I.; Tutuc, E.; *et al.* Large-Area Synthesis of High-Quality and Uniform Graphene Films on Copper Foils. *Science* **2009**, *324*, 1312–1314.
11. Zhao, J.; Pei, S.; Ren, W.; Gao, L.; Cheng, H.-M. Efficient Preparation of Large-Area Graphene Oxide Sheets for Transparent Conductive Films. *ACS Nano* **2010**, *4*, 5245–5252.
12. Luo, Z.; Lu, Y.; Somers, L. A.; Johnson, A. T. C. High Yield Preparation of Macroscopic Graphene Oxide Membranes. *J. Am. Chem. Soc.* **2009**, *131*, 898–899.
13. Liu, Z.; Wang, Z. M.; Yang, X.; Ooi, K. Intercalation of Organic Ammonium Ions into Layered Graphite Oxide. *Langmuir* **2002**, *18*, 4926–4932.
14. Zhang, K.; Mao, L.; Zhang, L. L.; Chan, H. S. O.; Zhao, X. S.; Wu, J. Surfactant-Intercalated, Chemically Reduced Graphene Oxide for High Performance Supercapacitor Electrodes. *J. Mater. Chem.* **2011**, *21*, 7302–7307.
15. Kovtyukhova, N. I.; Ollivier, P. J.; Martin, B. R.; Mallouk, T. E.; Chizhik, S. A.; Buzaneva, E. V.; Gorchinskiy, A. D. Layer-by-Layer Assembly of Ultrathin Composite Films from Micron-Sized Graphite Oxide Sheets and Polycations. *Chem. Mater.* **1999**, *11*, 771–778.
16. Wang, Y.; Xie, L.; Sha, J.; Ma, Y.; Han, J.; Dong, S.; Liu, H.; Fang, C.; Gong, S.; Wu, Z. Preparation and Chemical Reduction of Laurylamine-Intercalated Graphite Oxide. *J. Mater. Sci.* **2011**, *46*, 3611–3621.
17. Dikin, D. A.; Stankovich, S.; Zimney, E. J.; Piner, R. D.; Dommett, G. H. B.; Evmenenko, G.; Nguyen, S. T.; Ruoff, R. S. Preparation and Characterization of Graphene Oxide Paper. *Nature* **2007**, *448*, 457–460.
18. Xu, Y.; Bai, H.; Lu, G.; Li, C.; Shi, G. Flexible Graphene Films *via* the Filtration of Water-Soluble Noncovalent Functionalized Graphene Sheets. *J. Am. Chem. Soc.* **2008**, *130*, 5856–5857.
19. Kong, B.-S.; Yoo, H.-W.; Jung, H.-T. Electrical Conductivity of Graphene Films with a Poly(allylamine hydrochloride) Supporting Layer. *Langmuir* **2009**, *25*, 11008–11013.
20. Wang, X.; Zhi, L.; Mullen, K. Transparent, Conductive Graphene Electrodes for Dye-Sensitized Solar Cells. *Nano Lett.* **2007**, *8*, 323–327.
21. Zhu, Y.; Cai, W.; Piner, R. D.; Velamakanni, A.; Ruoff, R. S. Transparent Self-Assembled Films of Reduced Graphene Oxide Platelets. *Appl. Phys. Lett.* **2009**, *95*, 103104–103104−3.
22. Yamaguchi, H.; Eda, G.; Mattevi, C.; Kim, H.; Chhowalla, M. Highly Uniform 300 mm Wafer-Scale Deposition of Single and Multilayered Chemically Derived Graphene Thin Films. *ACS Nano* **2010**, *4*, 524–528.
23. Wang, X.; Zhi, L.; Tsao, N.; Tomović, Ž.; Li, J.; Müllen, K. Transparent Carbon Films as Electrodes in Organic Solar Cells. *Angew. Chem., Int. Ed.* **2008**, *47*, 2990–2992.
24. Becerril, H. A.; Mao, J.; Liu, Z.; Stoltenberg, R. M.; Bao, Z.; Chen, Y. Evaluation of Solution-Processed Reduced Graphene Oxide Films as Transparent Conductors. *ACS Nano* **2008**, *2*, 463–470.
25. Liang, Y.; Frisch, J.; Zhi, L.; Norouzi-Arasi, H.; Feng, X.; Rabe, J. P.; Koch, N.; Müllen, K. Transparent, Highly Conductive Graphene Electrodes from Acetylene-Assisted Thermolysis of Graphite Oxide Sheets and Nanographene Molecules. *Nanotechnology* **2009**, *20*, 434007.
26. Lee, D. W.; Hong, T.-K.; Kang, D.; Lee, J.; Heo, M.; Kim, J. Y.; Kim, B.-S.; Shin, H. S. Highly Controllable Transparent and

Conducting Thin Films Using Layer-by-Layer Assembly of Oppositely Charged Reduced Graphene Oxides. *J. Mat. Chem.* **2011**, *21*, 3438–3442.
27. Cote, L. J.; Kim, F.; Huang, J. Langmuir–Blodgett Assembly of Graphite Oxide Single Layers. *J. Am. Chem. Soc.* **2008**, *131*, 1043–1049.
28. Li, X.; Zhang, G.; Bai, X.; Sun, X.; Wang, X.; Wang, E.; Dai, H. Highly Conducting Graphene Sheets and Langmuir–Blodgett Films. *Nat. Nanotechnol.* **2008**, *3*, 538–542.
29. Ang, P. K.; Wang, S.; Bao, Q.; Thong, J. T. L.; Loh, K. P. High-Throughput Synthesis of Graphene by Intercalation–Exfoliation of Graphite Oxide and Study of Ionic Screening in Graphene Transistor. *ACS Nano* **2009**, *3*, 3587–3594.
30. Kaschak, D. M.; Johnson, S. A.; Hooks, D. E.; Kim, H.-N.; Ward, M. D.; Mallouk, T. E. Chemistry on the Edge: A Microscopic Analysis of the Intercalation, Exfoliation, Edge Functionalization, and Monolayer Surface Tiling Reactions of α-Zirconium Phosphate. *J. Am. Chem. Soc.* **1998**, *120*, 10887–10894.
31. Liu, Z.-h.; Wang, Z.-M.; Yang, X.; Ooi, K. Intercalation of Organic Ammonium Ions into Layered Graphite Oxide. *Langmuir* **2002**, *18*, 4926–4932.
32. Pan, S.; Aksay, I. A. Factors Controlling the Size of Graphene Oxide Sheets Produced *via* the Graphite Oxide Route. *ACS Nano* **2011**, *5*, 4073–4083.
33. Eda, G.; Fanchini, G.; Chhowalla, M. Large-Area Ultrathin Films of Reduced Graphene Oxide as a Transparent and Flexible Electronic Material. *Nat. Nanotechnol.* **2008**, *3*, 270–274.
34. Dang, T. T.; Pham, V. H.; Hur, S. H.; Kim, E. J.; Kong, B. S.; Chung, J. S. Superior Dispersion of Highly Reduced Graphene Oxide in N,N-dimethylformamide. *J. Colloid Interface Sci.* **2012**, *376*, 91–96.
35. Gómez-Navarro, C.; Weitz, R. T.; Bittner, A. M.; Scolari, M.; Mews, A.; Burghard, M.; Kern, K. Electronic Transport Properties of Individual Chemically Reduced Graphene Oxide Sheets. *Nano Lett.* **2007**, *7*, 3499–3503.
36. Sirisaksoontorn, W.; Adenuga, A. A.; Remcho, V. T.; Lerner, M. M. Preparation and Characterization of a Tetrabutylammonium Graphite Intercalation Compound. *J. Am. Chem. Soc.* **2011**, *133*, 12436–12438.
37. Park, K. H.; Kim, B. H.; Song, S. H.; Kwon, J.; Kong, B. S.; Kang, K.; Jeon, S. Exfoliation of Non-Oxidized Graphene Flakes for Scalable Conductive Film. *Nano Lett.* **2012**, *12*, 2871–2876.
38. Kim, J.; Cote, L. J.; Kim, F.; Yuan, W.; Shull, K. R.; Huang, J. Graphene Oxide Sheets at Interfaces. *J. Am. Chem. Soc.* **2010**, *132*, 8180–8186.
39. Umemura, J.; Kamata, T.; Kawai, T.; Takenaka, T. Quantitative Evaluation of Molecular Orientation in Thin Langmuir-Blodgett Films by FT-IR Transmission and Reflection-Absorption Spectroscopy. *J. Phys. Chem.* **1990**, *94*, 62–67.
40. Shin, H. S.; Jung, Y. M.; Lee, J.; Chang, T.; Ozaki, Y.; Kim, S. B. Structural Comparison of Langmuir-Blodgett and Spin-Coated Films of Poly(*tert*-butyl Methacrylate) by External Reflection FTIR Spectroscopy and Two-Dimensional Correlation Analysis. *Langmuir* **2002**, *18*, 5523–5528.